# Image De-noising based on the Statistical Modeling of Wavelet Coefficients and Quad-Tree Decomposition

J.N. Ellinas
*Technological Educational Institute of Piraeus, 12244*
*Egaleo, Greece*
*jellin@teipir.gr*

D. E. Manolakis
*Technological Educational Institute of Thessaloniki, 57400*
*Thessaloniki, Greece*
*dmanol@teithe.gr*

***Abstract* - This paper proposes a spatially adaptive statistical model for wavelet image coefficients in order to perform image de-noising. The wavelet coefficients are modelled as zero-mean Gaussian random variables with high local correlation. This model is developed in a Bayesian framework, where a Maximum Likelihood (ML) estimator evaluates the variance of the blocks to which the wavelet subbands have been segmented. Then, applying the Minimum Mean Squared Error (MMSE) estimation procedure, the original or de-noised wavelet image coefficients are estimated. The reliable estimation of local variance is performed by making the assumption that variance is locally smooth. The validity of this assumption is boosted by segmenting the wavelet subbands into blocks of variable size with two methods. The first method employs image quad-tree decomposition and transfers linearly the resulted tree on the wavelet subbands. This decomposition identifies object boundaries and defines more accurately the regions of smooth variance instead of dividing them in to blocks of fixed size. The second method performs quad-tree decomposition of every subband with a variance splitting criterion. The subbands are segmented into blocks of nearly constant variance, so that the transform coefficients to be approximated as i.i.d random variables. The extensive experimental evaluation shows that the proposed scheme demonstrates very good performance as far as PSNR measures and visual quality are concerned with respect to others state of the art de-noising schemes.**

***Index terms* - wavelets, de-noising, quad-tree decomposition.**

## I. INTRODUCTION

An image is often corrupted by noise during its acquisition or transmission. Image de-noising is used to remove the additive noise while retaining as much as possible the important image features. In the recent years there has been a fair amount of research on filtering and wavelet coefficients thresholding, because wavelets provide an appropriate basis for separating noisy signal from the image signal. These wavelet-based methods mainly rely on thresholding the Discrete Wavelet Transform (DWT) coefficients, which have been affected by Additive White Gaussian Noise (AWGN).

Since the work of Donoho and Johnstone [1]-[4], there has been a lot of research on the way of defining the threshold levels and their type (i.e. hard or soft threshold). These algorithms usually perform global thresholding of wavelet coefficients by retaining only large coefficients and setting the rest to zero. Thus, they do not present spatial adaptivity and their performance in real life images is not sufficiently effective.

A wide class of image processing algorithms is based on the DWT. The transform coefficients within the subbands can be locally modelled as independent identically distributed (i.i.d) random variables with Generalized Gaussian Distribution (GGD) [5]. In that sense, the de-noised coefficients may be evaluated by an MMSE (Minimum Mean Square Error) estimator, in terms of the noised coefficients and the variances of signal and noise. The signal variance is locally estimated by an ML (Maximum Likelihood) estimator, whereas noise variance is estimated from the first level diagonal details. Therefore, the de-noised coefficients are statistically estimated in small regions for every subband instead of applying a global threshold [6]. These methods present efficient results but their spatial adaptivity is not well suited near object edges where the variance field is not smoothly varied. In [7] a similar spatially adaptive model for wavelet image coefficients was used to perform image de-noising via wavelet thresholding.

The present work employs the spatially adaptive model as in [6] and performs MMSE coefficient estimation, rather than coefficient thresholding as in [7]. However, it differs from [6] in the way that the underlying variance field is estimated. In our work, this estimation is performed in a variable block size framework in contradiction to [6] where a fixed block size framework is used. The subbands segmentation into blocks of variable size is performed with two methods. The first method decomposes the noisy image by employing quad-tree analysis and transfers linearly the resulted tree on the wavelet subbands. This approximation is rational if the spatial dependency among the image and the wavelet subbands is considered. This decomposition identifies object boundaries and defines more accurately the regions of smooth variance instead of dividing them in to blocks of standard size. In addition, the algorithm becomes faster as fewer blocks are created. The second method decomposes every subband employing quad-tree analysis with a variance splitting criterion. The subbands are segmented into blocks of nearly constant variance, so that the transform coefficients to be approximated as i.i.d random variables.

This paper is organized as follows. Section 2 describes the proposed de-noising algorithm. The experimental results are presented in Section 3 and the conclusions are summarized in Section 4.

## II. THE PROPOSED DE-NOISING ALGORITHM

### *A. The statistical model*

The statistical model of the proposed de-noising algorithm is illustrated in Fig. 1. A noise contaminated image may be formulated as in the block-diagram. A "clean" image, $x$, is decomposed by DWT providing the wavelet coefficients $X$(k). These coefficients, which may be locally considered as i.i.d GGD random variables with variance $\sigma_X^2(k)$, are corrupted by additive i.i.d Gaussian noise samples, $n$(k), to produce the observed wavelet coefficients of the noisy image, $Y$(k).

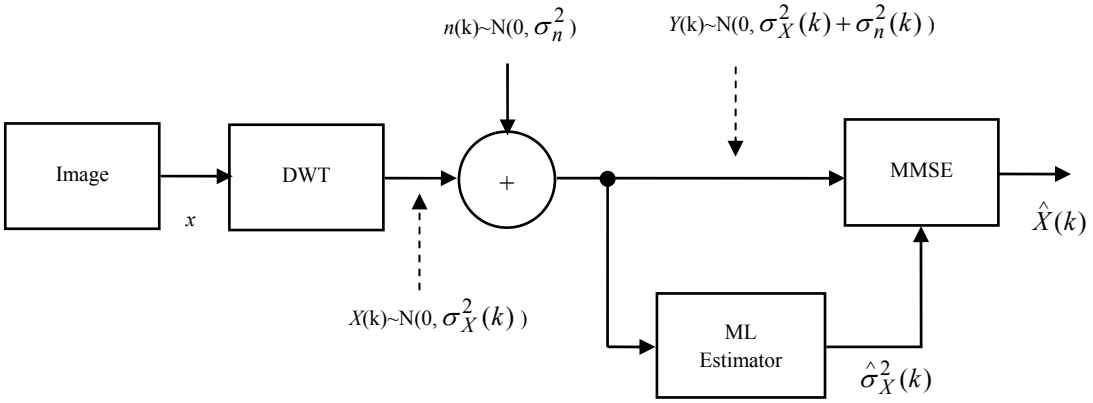


**Fig. 1** Block-diagram of the proposed de-noising algorithm. The statistical model is based on an ML estimator for an estimate of the underlying variance and an MMSE estimator for the evaluation of the "clean" wavelet coefficients.

Let $W$ and $W^{-1}$ denote the two dimensional DWT and its inverse respectively. The relationship between image and transform coefficients is:

$$X = Wx \quad and \quad x = W^{-1}X \tag{1}$$

The "clean" coefficients, $X$, may be estimated from the observed coefficients, $Y$, if noise variance, $\sigma_n^2$ and image variance, $\sigma_X^2(k)$ are known. Here, a robust median estimator of the highest subband diagonal coefficients (i.e. $HH_1$) estimates the noise variance [2]. Also, an ML estimation of image variance is performed for every transform coefficient, using the observed noisy data in its local neighborhood. In this work, the local neighborhood is defined by segmenting the image or every subband by quad-tree decomposition. Finally, an MMSE estimator provides an estimate of the "clean" coefficients, $\hat{X}(k)$. The reconstructed de-noised image is given by:

$$\hat{x} = W^{-1}\hat{X} \tag{2}$$

### *B. The mathematical estimation*

It is known that the best estimate of a random variable $x$ given by an MMSE estimator is:

$$\hat{X} = E[X] \tag{3}$$

Also, under the assumptions of independence and Gaussian distribution of the random variables, it is known that [8]:

$$\begin{aligned} f_X &\sim N(0, \sigma_X^2) \\ f_Y &\sim N(0, \sigma_X^2 + \sigma_n^2) \\ f_{Y|X} &\sim N(x, \sigma_n^2) \end{aligned} \tag{4}$$

The last equation describes the conditional distribution of the observed values when the "clean" values are known. The Bayesian estimation of the "clean" values given the observed values is:

$$f_{X|Y} = \frac{f_{Y|X}\, f_X}{f_Y} = \frac{N(x, \sigma_n^2)\, N(0, \sigma_X^2)}{N(0, \sigma_X^2 + \sigma_n^2)} \tag{5}$$

If the Gaussian distributions are replaced by their explicit forms, equation (5) results in:

$$f_{X|Y} \sim N\left(\frac{\sigma_X^2}{\sigma_X^2 + \sigma_n^2} y, \frac{\sigma_X^2 \sigma_n^2}{\sigma_X^2 + \sigma_n^2}\right) \tag{6}$$

The estimated "clean" wavelet coefficients result by considering equations (3) and (6):

$$\hat{X}(k) = \frac{\sigma_X^2}{\sigma_X^2 + \sigma_n^2} Y(k) \quad (7)$$

But in fact $\sigma_X^2$ is not known, so we employ an ML estimator in order to have an estimate, $\hat{\sigma}_X^2$, for a local neighborhood, where variance is assumed to be constant. The ML estimate is defined as:

$$\hat{X}_{ML}(y) = \arg\max_x f_{Y|X}(y \mid x) \quad (8)$$

In our case, this takes the following form:

$$\hat{X}_{ML}(y) = \arg\max_{\sigma_y^2} \prod_{j \in \mathcal{N}} f(y, \sigma_y^2) \quad (9)$$

where $\mathcal{N}$ is the local neighborhood. The maximum of the above equation is found to be for:

$$\sigma_y^2 = \frac{1}{M} \sum_{k=1}^{M} Y^2(k) \quad (10)$$

where $M$ represents the number of wavelet coefficients residing in the local neighborhood $\mathcal{N}$.
Therefore, the estimate of the "clean" coefficients variance is:

$$\hat{\sigma}_X^2 = \frac{1}{M} \sum_{k=1}^{M} Y^2(k) - \sigma_n^2 \quad (11)$$

Finally, the "clean" coefficients are estimated combining (7) and (11):

$$\hat{X}(k) = \frac{\hat{\sigma}_X^2}{\hat{\sigma}_X^2 + \sigma_n^2} Y(k) \quad (12)$$

where the noise variance is estimated, as it was stated in the previous subsection, by:

$$\sigma_n^2 = \left[ \frac{median(|Y(k)|)}{0.6745} \right]^2 \quad (13)$$

where $Y(k)$ represent the coefficients of $HH_1$ subband.

### *C. The proposed methods of de-noising*

Applying the aforementioned analysis, the noise contaminated image is subjected to DWT and the "clean" coefficients are estimated by equations (11), (12) and (13). Then, the "clean" image is attained by reconstruction employing the inverse DWT. However, the above mentioned equations are valid assuming that the underlying variance field in the subbands is varying smoothly in a local neighbourhood. The local neighbourhood may be defined by segmenting the subbands into blocks of fixed size [6] or into blocks of variable size as it is proposed in this work.

The first method of segmentation is based on quad-tree decomposition (QTD) of the noisy image applying an intensity difference splitting criterion. According to this criterion, a parent block splits into four children blocks if the intensity gradient within block is greater than a predefined threshold. Fig. 2 illustrates the segmentation of "Lena" image and its associated horizontal subband with QTD.

**Fig. 2** QTD segmentation into blocks of variable size. (a) Noisy image; (b) Horizontal subband ($HL_1$) after DWT.

The image is transformed by DWT and the segmentation tree is linearly transferred in every subband because there is a spatial dependency among the subbands and the image. This decomposition identifies object boundaries and defines more accurately the regions of smooth variance instead of dividing them in to blocks of fixed size. Also, the computational complexity is lowered because the execution of the algorithm is performed in fewer blocks.

The second method transforms the image by DWT and segments each subband by QTD employing a variance splitting criterion, Fig. 3. According to this criterion, a parent block splits into four children blocks if its variance is greater than a predefined threshold. The threshold is set to a low value so that the resulting blocks to present uniform variance. In this work, the variance threshold is set to 10% of the subband's variance.

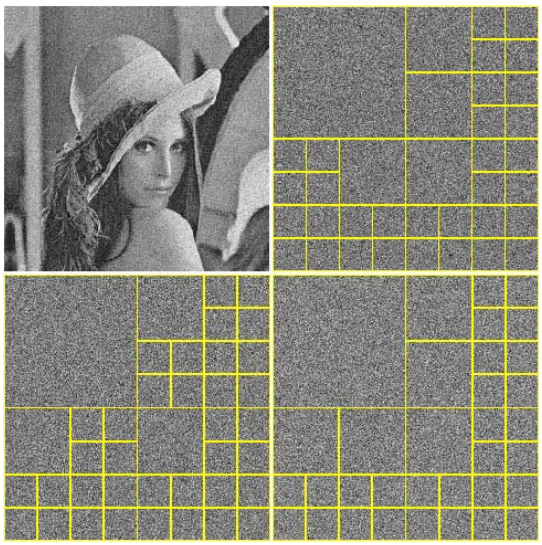

**Fig. 3** Subbands QTD segmentation into blocks of variable size.

## III. EXPERIMENTAL RESULTS

The experimental evaluation is performed on three gray scale images like "Lena", "Barbara" and "Boat" of size 512×512 pixels at different noise levels. The wavelet transform employs Daubechies's least asymmetric compactly supported wavelet with eight vanishing moments [9] at four levels of decomposition. The objective quality of the reconstructed image is measured by:

$$PSNR = 10\log_{10}\frac{255^2}{mse}\ \text{dB} \qquad (14)$$

where *mse* is the mean square error between the original (i.e. $x$) and the de-noised image (i.e. $\hat{x}$) with size $I$x$J$:

$$mse = \frac{1}{IxJ}\sum_{i=1}^{I}\sum_{j=1}^{J}[x(i,j) - x(\hat{i},j)]^2 \qquad (15)$$

To assess the performance of our first proposed method, it is compared with *SureShrink* [3], *BayesShrink* [7], *NormalShrink* [10], *Wiener* [11] and *LAWML* [6]. The first of the above mentioned methods is the hard-thresholding of wavelet coefficients using a constant threshold for all subbands that is estimated by a robust estimator from $HH_1$ subband. The second method uses spatially adaptive wavelet thresholding. The third method employs the same principle as the previous one in order to estimate subband dependent threshold. The fourth method is based on the Wiener filter de-noising algorithm and the last one employs the statistical modelling of wavelet coefficients in order to estimate the "clean" coefficients using the observed ones and estimating the underlying variance field in a local neighbourhood. The PSNR of the various methods are compared in Table I and the best ones are highlighted in bold fonts.

**TABLE I**
PSNR comparative results for "Lena" and various values of noise standard deviation.

| | **SureShrink** | **BayesShrink** | **NormalShrink** | **Wiener** | **LAWML** | **QTD** |
|---|---|---|---|---|---|---|
| **Lena** | | | | | | |
| $\sigma_n$=10 | 33.34 | 33.16 | 32.80 | 33.59 | **33.87** | 33.60 |
| $\sigma_n$=15 | 31.22 | 31.18 | 30.89 | 31.12 | **31.58** | 31.52 |
| $\sigma_n$=20 | 29.80 | 29.82 | 29.60 | 28.99 | 29.91 | **30.17** |
| $\sigma_n$=25 | 28.67 | 28.87 | 28.54 | 27.19 | 28.56 | **29.11** |
| $\sigma_n$=30 | 28.07 | **28.12** | 27.72 | 25.67 | 27.62 | 28.07 |

(a) (b) (c) (d)

**Fig. 4** Subjective quality performance comparison for noise standard deviation $\sigma_n$=30.
(a) Noisy image; (b) *SureShrink*; (c) *BayesShrink*; (d) *QTD*.

It is apparent that our first proposed method, called *QTD*, performs at least equally well to all other methods in almost the whole examining range. Fig. 4 demonstrates the subjective quality performance among the three methods that present the best PSNR results from Table I. In this figure, "Lena" is contaminated with noise of standard deviation equal to 30. It may be observed that the quality of the de-noised image of our proposed method is quite fair compared to *SureShrink* and *BayesShrink*, both in low and high textured areas.

The performance of our second proposed method, called *QTDvar*, is compared with the previous *QTD* method, *LAWML* and *BayesShrink*. Tables II, III and IV provide the comparative results of these methods for the three tested images. Our method provides considerable PSNR margins over the other algorithms. For example, in "Lena" *QTDvar* outperforms *LAWML* by 1.5 dB and *BayesShrink* by 1 dB for $\sigma_n$=30, that is, in a heavily noise contaminated image. Similarly, in "Barbara" *QTDvar* outperforms *LAWML* by 0.18 dB and *BayesShrink* by 1 dB for $\sigma_n$=30. In "Boat", there is a better objective quality by 0.7 dB for $\sigma_n$=30.

Fig. 5 illustrates the quality performance of the above methods for "Boat" image, which is affected with noise of $\sigma_n$=30. It is obvious that *QTDvar* method performs better de-noising than the other methods and provides a more pleasant image quality, in a strong additive noise environment.

**TABLE II**
PSNR comparative results for "Lena" image and various values of noise standard deviation.

| | **BayesShrink** | **LAWML** | **QTD** | **QTDvar** |
|---|---|---|---|---|
| **Lena** | | | | |
| $\sigma_n$=10 | 33.16 | 33.87 | 33.60 | **34.03** |
| $\sigma_n$=15 | 31.18 | 31.58 | 31.52 | **32.22** |
| $\sigma_n$=20 | 29.82 | 29.91 | 30.17 | **30.92** |
| $\sigma_n$=25 | 28.87 | 28.56 | 29.11 | **29.91** |
| $\sigma_n$=30 | 28.12 | 27.62 | 28.07 | **29.11** |

**TABLE III**
PSNR comparative results for "Barbara" image and various values of noise standard deviation.

| | **BayesShrink** | **LAWML** | **QTD** | **QTDvar** |
|---|---|---|---|---|
| **Barbara** | | | | |
| $\sigma_n$=10 | 31.21 | **32.47** | 31.18 | 31.77 |
| $\sigma_n$=15 | 28.72 | **30.08** | 29.36 | 29.58 |
| $\sigma_n$=20 | 27.18 | **28.35** | 27.96 | 28.11 |
| $\sigma_n$=25 | 26.08 | 27.07 | 26.93 | **27.08** |
| $\sigma_n$=30 | 25.20 | 26.00 | 26.01 | **26.18** |

**TABLE IV**
PSNR comparative results for "Boat" image and various values of noise standard deviation.

| | **BayesShrink** | **LAWML** | **QTD** | **QTDvar** |
|---|---|---|---|---|
| **Boat** | | | | |
| $\sigma_n$=10 | 31.82 | **32.39** | 31.67 | 32.06 |
| $\sigma_n$=15 | 29.65 | **30.15** | 29.83 | 30.12 |
| $\sigma_n$=20 | 28.20 | 28.56 | 28.48 | **28.77** |
| $\sigma_n$=25 | 27.19 | 27.34 | 27.46 | **27.80** |
| $\sigma_n$=30 | 26.37 | 26.31 | 26.59 | **27.05** |

Fig. 6 shows the subjective quality of the two best methods, which are our proposed method *QTDvar* and *LAWML*, for "Barbara". The noise standard deviation is set again to $\sigma_n$=30. The reconstructed images have been magnified in order to observe differences around a region that contains low and high texture areas.

It may be observed that our proposed algorithm *QTDvar* performs equally well to *LAWML* around the kerchief stripes of "Barbara" and outperforms *LAWML* around her face, where the reconstructed image has smoother texture. Thus, our algorithms perform very efficiently in both low and high textured areas in a high interfering environment.

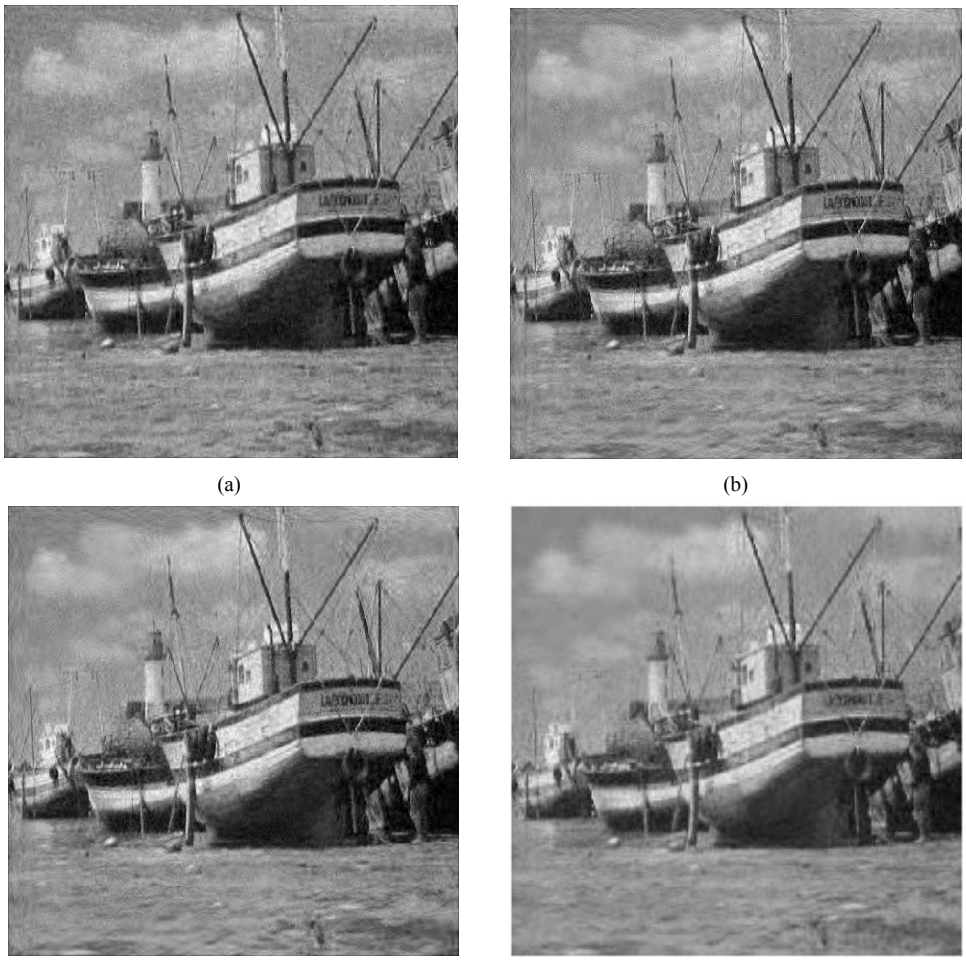

(a) (b)

(c) (d)

**Fig. 5** Subjective quality performance comparison for noise standard deviation $\sigma_n$=30.
(a) *BayesShrink*; (b) *LAWML*; (c) *QTD*; (d) *QTDvar*.

(a) (b)

**Fig. 6** Subjective quality performance comparison for noise standard deviation $\sigma_n$=30.
(a) *LAWML*; (b) *QTDvar*.

## IV. CONCLUSIONS

In this paper, two methods are proposed for recovering an image from noise contamination effectively. They are based on the discrete wavelet decomposition of the image and the Generalized Gaussian Distribution modelling of the subband coefficients. Both methods employ a spatially adaptive model and perform MMSE coefficient estimation instead of the classical threshold estimation. The proposed algorithm segments the subbands into blocks of variable size and estimates the variance in each block assuming that it is smoothly varying in a local neighbourhood. The novelty of the proposed methods is that the local neighbourhood in the subbands are blocks of variable size. This ensures that the underlying variance field is more uniform and its estimation is more accurate. Moreover, there is an inherent edge preserving mechanism from over smoothing, as the object edges are confined in blocks of small size. The segmentation is performed by quad-tree decomposition employing an intensity or variance splitting criterion. The noise variance is estimated by the robust estimator used by *SureShrink* method. Finally, the "clean" coefficients are estimated by an MMSE estimator and the "clean" image is recovered by an inverse transform.

The first proposed method decomposes the noisy image employing quad-tree analysis and transfers linearly the resulted tree on the wavelet subbands. This decomposition identifies object boundaries and defines more accurately the regions of smooth variance instead of dividing them in to blocks of standard size. The second method decomposes every subband employing quad-tree analysis with a variance splitting criterion. The subbands are segmented into blocks of nearly constant variance and the transform coefficients can be approximated as i.i.d random variables. The two proposed algorithms are tested with three grey scale images for various values of noise standard deviation and their performance is compared with other de-noising algorithms. The experimental evaluation showed that the proposed methods have a very good performance, providing reconstructed images with fairly good quality.


### ACKNOWLEDGMENTS

This work is co-funded by the European Social Fund & National Resources - EPEAEK II - ARCHIMIDIS II.


### REFERENCES


[1] D.L. Donoho, De-noising by soft thresholding, IEEE Trans. on Info. Theory, pp. 933-936, 1993.

[2] D.L. Donoho, I.M. Johnstone, Ideal spatial adaptation via wavelet shrinkage, Biometrica, vol. 81, pp. 425-455, 1994.

[3] D.L. Donoho, I.M. Johnstone, Adapting to unknown smoothness via wavelet shrinkage, Journal of American statistical assoc., vol. 90, no. 432, pp. 1200-1224, Dec. 1995.

[4] D.L. Donoho, I.M. Johnstone, Wavelet shrinkage: Asymptopia, J.R. Stat. Soc., series B, vol. 57, no. 2, pp. 301-369, 1995.

[5] S. Mallat, A theory for multiresolution signal decomposition: the wavelet representation, IEEE Trans. on Pattern Anal. Mach. Intell., vol. 11, pp. 674-693, July 1989.

[6] M. K. Mihcak, I. Kozintsev, K. Ramchandran, Spatially adaptive statistical modelling of wavelet image coefficients and its application to denoising, IEEE Intern. Conf. on Acoustics, Speech and Signal Processing, vol.6, pp. 3253-3256, March 1999.

[7] S. G. Chang, B. Yu and M. Vetterli, Adaptive wavelet thresholding for image denoising and compression, IEEE Trans. on Image Proc., vol. 9, no. 9, pp. 1532-1546, Sept. 2000.

[8] R. M. Gray, L. D. Davisson, An introduction to statistical signal processing, Stanford University, 1999.

[9] I. Daubechies, Ten lectures on wavelets, Proceedings CBMS-NSF Regional Conference Series in Applied Mathematics, SIAM, vol. 61, 1992.

[10] L. Kaur, S. Gupta, R.C.Chauhan, "Image denoising using wavelet thresholding", Indian Conference on computer Vision, Graphics and Image Processing, Ahmedabad, Dec. 2002.

[11] Mathworks Inc., Matlab, Image Processing Toolbox.